View metadata, citation and similar papers at core.ac.uk

brought to you by CORE

provided by Caltech Authors - Main

Copyright WILEY-VCH Verlag GmbH & Co. KGaA, 69469 Weinheim, Germany, 2019.

NANO MICRO small

Supporting Information

for *Small,* DOI: 10.1002/smll.201804385

Noninvasive Featherlight Wearable Compliant "Marine Skin": Standalone Multisensory System for Deep-Sea Environmental Monitoring

*Sohail F. Shaikh, Harold F. Mazo-Mantilla, Nadeem Qaiser, Sherjeel M. Khan, Joanna M. Nassar, Nathan R. Geraldi, Carlos M. Duarte, and Muhammad M. Hussain**

Supporting Information

Title: Non-invasive featherlight wearable compliant "Marine Skin" – standalone multi-sensory system for deep-sea environment monitoring

Sohail F. Shaikh[1], Harold F. Mazo-Mantilla[1], Nadeem Qaiser[1], Sherjeel M. Khan[1], Joanna M. Nassar[2], Nathan R. Geraldi[3], Carlos M. Duarte[3], and Muhammad M. Hussain[1]*

[1]mmh Labs, Electrical Engineering, Computer Electrical Mathematical Science and Engineering Division (CEMSE), King Abdullah University of Science and Technology (KAUST), Thuwal 23955-6900, Saudi Arabia.
[2]California Institute of Technology, Pasadena, CA 91125, USA.
[3]Red Sea Research Center (RSRC), Division of Biological and Environmental Sciences and Engineering (BESE), King Abdullah University of Science and Technology (KAUST), Thuwal 23955-6900, Saudi Arabia.

*Corresponding author's e-mail: muhammadmustafa.hussain@kaust.edu.sa

Keywords: marine ecology, flexible systems, non-invasive tag, soft packaging, hybrid integration,

1. Material and Design Optimisation

1.1. Temperature Sensor

Oceanic temperature is relatively stable in response to changes in climates, for example, the change in oceanic temperature is effectively 0.1 °C for 0.6 °C change in global average temperature in the last century. However, the temperature of the seawater varies with the increasing depth (200-1500 m) known as thermocline region, which also has a significant effect on the marine ecosystems at different depths. [1–4] We compare the performance of the temperature sensor with the performance of the commercial temperature sensor integrated circuit (IC) from Sensirion. Commercial temperature sensor IC from Sensirion is attached to next to the fabricated temperature sensor on the wafer for accurate temperature detection. Both the reference and test sensors are subjected to heating from room temperature of 21 °C all the way up to 80 °C using a hot air gun. Initially, both the sensors record the values for room temperature which starts

increasing as the hot air gun is brought closer and closer to the sensor gradually. From **Figure S1**, we can clearly observe that change in resistance of version 2 sensor follows exactly with the reference standard. Instantaneous variations in the resistance change not only suggest that the resolution is high but also the response and recovery times match are at least on par with the status quo if not better.

1.2. Salinity Sensor

Similarly, the salinity of the seawater is fairly constant at the surface and at greater depths (> 800 m) but it varies rapidly in the halocline region (the region of rapid change of salinity, ~ 300 – 1000 m) similar to thermocline region for temperature. Variations in the oceanic salinity have been reported to affect the water cycles and the oceanic circulation. Factors that increase the salinity gradually of the oceanic surface are naturally counterbalanced by the inflow of fresh water from rivers, global ice melting, and precipitation of rainwater.[5,6] Ocean surface salinity is also one of the key parameters in understanding the effects of freshwater intake on the ocean dynamics due to occurrences of 86% evaporation and 78% global precipitation over the ocean. Thus, quantifying temperature and salinity can provide us with the basic understanding of the adaptability, habitat, food habits and growth profiles of the marine species. In addition, the density of seawater varies with the variation in temperature, depth, and the salinity. Variations in the density of water are significantly observed in pycnocline region (~ 200 – 500 m) (a subset of the halocline and thermocline regions) whereas, the density variation saturates at depths beyond 1000 m. [2,5] Conventionally, a salinity sensor is a simple 2 electrode design separated by some distance (2 mm in our first version). To increase the stability and the sensitivity, we have modified the design to interdigitated electrode pattern and hence observed more than ~625% increase in the sensitivity with stable and robust performance (**Figure S2**). We also observed ~135% increment in the sensitivity due to change of material from Au to Cu (**Figure S2b**),

however, an effect has been neglected due to corrosive nature of Cu which can degrade the performance of exposed salinity sensor underwater.

1.3. Pressure Sensor

The underwater pressure of the oceanic environment is directly related to the height of the water ($\boldsymbol{P = \rho \cdot h \cdot g}$) where **P** is the hydrostatic pressure, $\boldsymbol{\rho}$ is the density of water, **g**-acceleration due to gravity, and **h**-represents the height of water. The total pressure exerted ($\mathbf{P_{total}}$) on any object underwater is the combination of partial hydrostatic pressure **P** and the atmospheric pressure ($\mathbf{P_0}$), ($\boldsymbol{P_{total} = P + P_0}$) at the sea level which measures 14 psi for each atmospheric pressure. Conventional pressure sensors have high sensitivity with a caveat of low operating range, which restricts the usage in the marine sensors. Hence, we have designed our depth sensor based on a parallel plate capacitance principle where the capacitance varies linearly with the increasing depth with extremely good sensitivity and instantaneously. We chose PDMS due to its compressive nature as a dielectric material for capacitive pressure monitoring underwater. Due to its inherent compressive nature, we could use it as a dielectric material that can change the thickness on pressure application and hence the capacitance change is detected in response to the pressure. PDMS is prepared by mixing the elastomer to curing agent in the ratio of (10:1) is cured mostly at 90 °C for 60 minutes. However, altering the mixing ratio and curing temperature modifies the compressibility and elasticity of PDMS. To improve the compressibility of the dielectric layer, we modified the PDMS elastomer to curing agent mixture during preparation. Increase in elastomer ratio (12:1) from (10:1) and curing at a relatively low temperature (60 °C) resulted in increased compressibility implying increased sensitivity. Also, the thickness of the dielectric layer plays an important role in having increasing the detection range of the pressure (or depth). We have observed higher sensitivity for 1:12 composition of PDMS (**Figure S3a**) whereas similar increment was observed for thickness of 50 µm (**Figure**

S3b). Our material choices and the optimisation has increased the operating range up to 2 km which was only restricted due to non-availability of the tool that can simulate higher pressure than equivalent to 2 km.

For depth measurements at a high-pressure environment, we used a hydraulic pressure simulation tool available in the lab. The tool has the capabilities to control the applied pressure in the chamber filled with water up to a maximum pressure of 3000 psi, which is equivalent to a depth of 2000 m. However, the recommended maximum value for applied pressure was 2300 psi for the equipment restricting our measurements to a maximum pressure equivalent to a depth of 1500 m (**Figure S4**). The experimental setup is shown in **Figure S4b** in which the sensor is immersed in a closed metallic vessel (~70 cm tall with an internal diameter of 15 cm) with thermal insulation from outside, connected to a digital and manual pressure control system. The simulation tool is a custom designed set-up that has 3 different components: pressure and temperature controller, hydraulic pump, and the chamber. The hydraulic pump is mainly for applying manual pressure (Figure S4b right inset). The applied pressure can be calibrated or readout using an analog dead weight measurement system (Ametek test & calibration instruments) or digital tools (Digiquartz Portable Standard from Paroscientific Inc.). The steel vessel that is filled with the seawater also has waterproof connectors that can be connected to other tools like Oscilloscope, function generator or any other electronic instrument. We started with digitally controlling the pressure applied through a small hydraulic hand-pump, however, observed a lot of noise in the recording of the signal. This noise was figured to be originating from the electrical interference of the connections of a digital control system to the steel vessel. We switched to manual control mode and applied pressure in an incremental way up to 1500 m with a step size of 30 m (~43 psi). Real-time variation in capacitance of pressure/depth sensor

with respect to the applied changing pressure has been plotted in Figure S3a. It can be seen that the sensor exhibits a linear relationship to the change in depth of the water with extremely fast response time. An incremental increase in the capacitance with the corresponding step increase in applied pressure appears to be constant throughout the entire range. From this response, it can be conferred that sensor performance neither degrade nor reach a saturation in the value, thereby can withstand the pressure of water higher than the depths of 2 km. One can observer oscillations in the capacitance change from **Figure S4**, with incremental pressure. These oscillations are arising from the decrease in the pressure during manual application of pressure, and hence the hydraulic pressure drops initially then ramps up to the desired values. These oscillations to the variations in the pressure experienced during the step increment confirm high sensitivity and the resolution of the depth sensor.

2. Rugged Performance Testing

2.1. Cyclic Bending Tests

For the reliability of the Marine Skin, it is important to study the effect of the harsh environmental parameters that it may experience. The two important parameters are high salinity exposure for extended periods (multiple weeks) and no degradation in the performance due to physical deformations. First, the ruggedness of the depth sensors and integrity of packaging were tested by subjecting the fabricated Marine Skin to a large number of bending cycles with the bending radius of 1 mm. Depth measurements in the lab environment are carried out after 100, 500, 1000, 2500, and 10^4 bending cycles (**Supplementary Video S1**). Real-time variations in the capacitance while submerging in the water in steps of 10 cm each plotted in **Figure S5** where the change in each step is consistent with the only variation due to the manual handling error in maintaining constant step height increment. The sharp increase in the capacitance occurs as soon as the sensor is immersed in water from the air. To confirm the reliability for the ruggedness over

different cycles, hysteresis tests are performed where measurements are recorded at specific depths during increasing depths (submerging) and decreasing depths (rising up) of water. **Figure S6** illustrates excellent hysteresis characteristics of the sensors the variation in depth, nevertheless, the variations in the hysteresis can also be attributed to variations occurring due to manual handling.

2.2. Prolonged Exposure to Saline Environment

Similarly, the packaging integrity is validated from the prolonged exposure of high salinity (41 PSU) Red Seawater on the sensors. We immersed the packaged Marine Skin platform in the seawater and measured the performance after 1 day, 3 days, 7 days, 15 days and 28 days to evaluate the integrity of packaging. The real-time change in the capacitance with increasing depth of the water is acquired (**Figure S7**) for these different scenarios, which show no degradation in terms of saturation or sensitivity. Thus, we can conclude that the integrity of packaging and the reliability of the sensors makes the Marine Skin platform an extremely robust, flexible, and highly lightweight solution for marine environmental monitoring.

3. Attachment Strategies and Wearable Bracelet Design

3.1. Attachment on Large Species

The tagging of the marine species has always been a non-invasive method involving incisions through skin, tissues, usage of metallic and plastic anchors inserted in the skin. Invasive method of attachment can lead to the injury of the species, which not only introduces great discomfort to the tagged individual but also can affect their normal movements and behavior. Thus, the requirement of 2% body weight of the bio-loggers, flexibility and non-invasive nature of the devices are under focus. Our focus was on making a flexible standalone system that can adhere to all these norms in addition to having a completely non-invasive tagging mechanism. In

past, Marine Skin version 1, was tested for its flexibility and non-invasive method attachment on tiger shark, wobbegong shark, and stingray (**Figure 7**). We mounted the sensors on a cylindrical CAN host attached to a steel clamp that was attached to the dorsal fin of the shark. This method can only be applicable to large species with the dorsal fin acting as an anchor for the sensing system. For other species with comparatively smoother and mucous skin or smaller sized animals, we needed to use other techniques. Superglue can be used on the species with hard shells (turtles, crab etc.) whereas as dental/surgical glue was tested on a wobbegong and Stingray (**Supplementary Video S3**). The hydrodynamic forces due to the stream of water detach the sensors from the body of the animal. Not only the water stream but also this glue is dissolvable in water in 48 hours making this method unsuitable for long-term deployment.

3.2. Wearable Bracelet Design

We designed a unique strategy of making a soft elastic wearable jacket (bracelet) like structure to host the sensors made from the same material. The wearable gadget can be wrapped around the species and its strong locking mechanism can prevent it from detachment due to water stream itself. We made 3D printed molds for replicating the wearable modules, followed by pouring PDMS to cure at 60 °C for an hour. This cured wearable jacket design embedded with the sensory platform can be easily peeled from the mold (**Figure S9**). In the initial design, we used the locking mechanism of soft-pins and the holes made from the same PDMS material (**Figure S9c**). However, the design of the soft pins was not strong enough to withstand the stream pressure, in addition, the adhesive strength was not sufficient to hold the jacket on the skin. We modified the design to incorporate a 3D printed pin structure for increasing the strength of the locking mechanism. These 3D printed mushroom pins provide excellent strength and hence the successful attachment on barramundi and seabream fishes can be seen in **video S4 and**

S5. Dental adhesive can be used on the inner lining of the soft wearable bracelet to reduce the friction between the elastic soft material and the skin and hence reducing the minuscule probability of injury due to this soft bracelet.

REFERENCES

[1] J. B. C. Jackson, M. X. Kirby, W. H. Berger, K. A. Bjorndal, L. W. Botsford, B. J. Bourque, R. H. Bradbury, R. Cooke, J. Erlandson, J. A. Estes, T. P. Hughes, S. Kidwell, C. B. Lange, H. S. Lenihan, J. M. Pandolfi, C. H. Peterson, R. S. Steneck, M. J. Tegner, R. R. Warner, Science (80-.). **2001**, 293, 629.

[2] USEPA, "Climate Change Indicators: Stream Temperature," can be found under https://www.epa.gov/climate-indicators/climate-change-indicators-sea-surface-temperature, **2016**.

[3] S. C. Doney, M. Ruckelshaus, J. Emmett Duffy, J. P. Barry, F. Chan, C. A. English, H. M. Galindo, J. M. Grebmeier, A. B. Hollowed, N. Knowlton, J. Polovina, N. N. Rabalais, W. J. Sydeman, L. D. Talley, Ann. Rev. Mar. Sci. **2012**, 4, 11.

[4] J. H. Koo, D. C. Kim, H. J. Shim, T. H. Kim, D. H. Kim, Adv. Funct. Mater. **2018**, DOI 10.1002/adfm.201801834.

[5] "Salinity | Science Mission Directorate," can be found under https://science.nasa.gov/earth-science/oceanography/physical-ocean/salinity, **n.d.** in Int. Geophys., **1994**, pp. 171–203.

SUPPORTING FIGURES

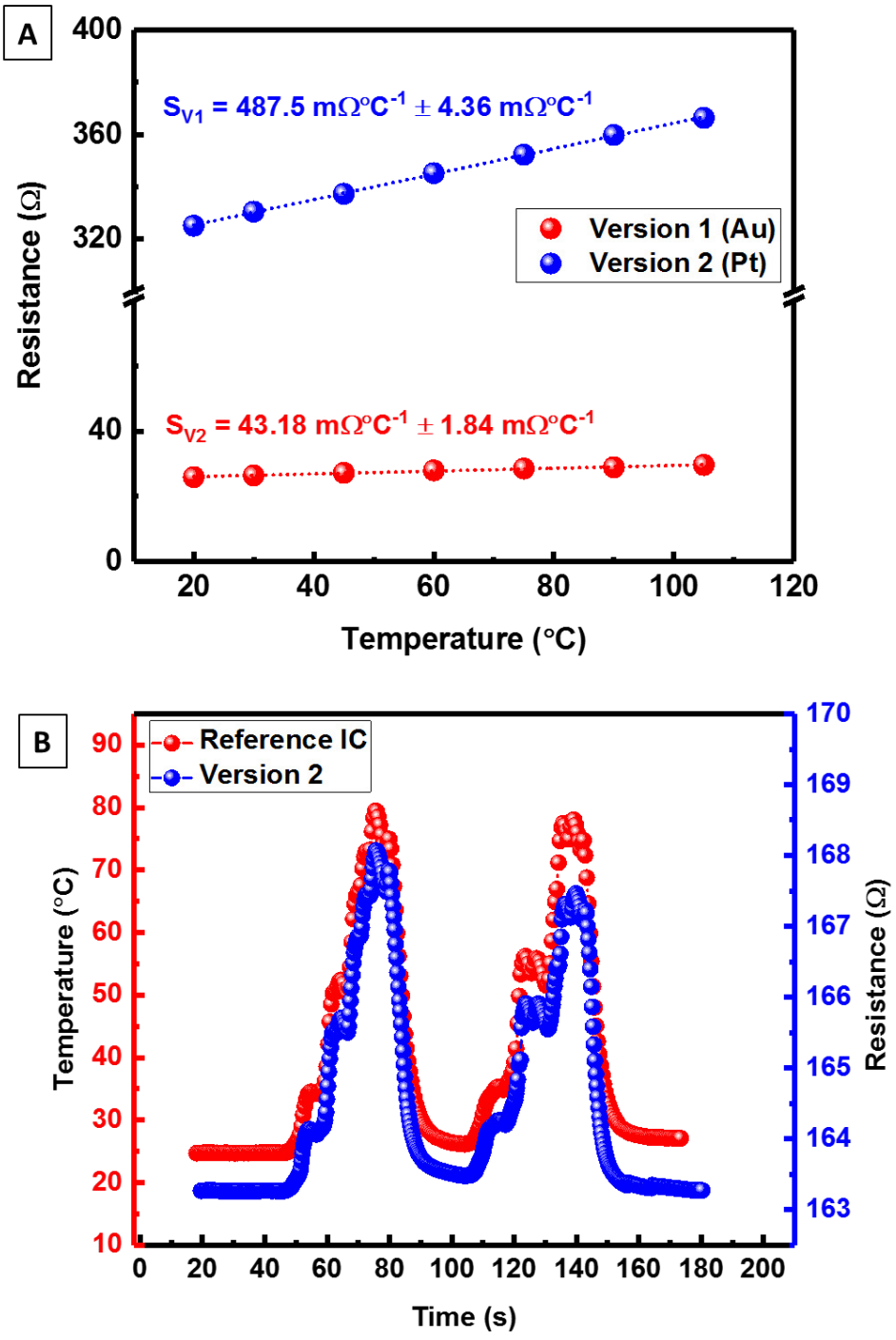

Figure S1: Comparison of the performance of (A) version 1 and version 2 temperature sensor for material choice and improved sensitivity, and (B)Version 2 comparison and calibration with

the commercial temperature sensor IC from Sensirion. Fabricated sensors changes the resistance corresponding to the temperature with the response exactly following the reference sensor.

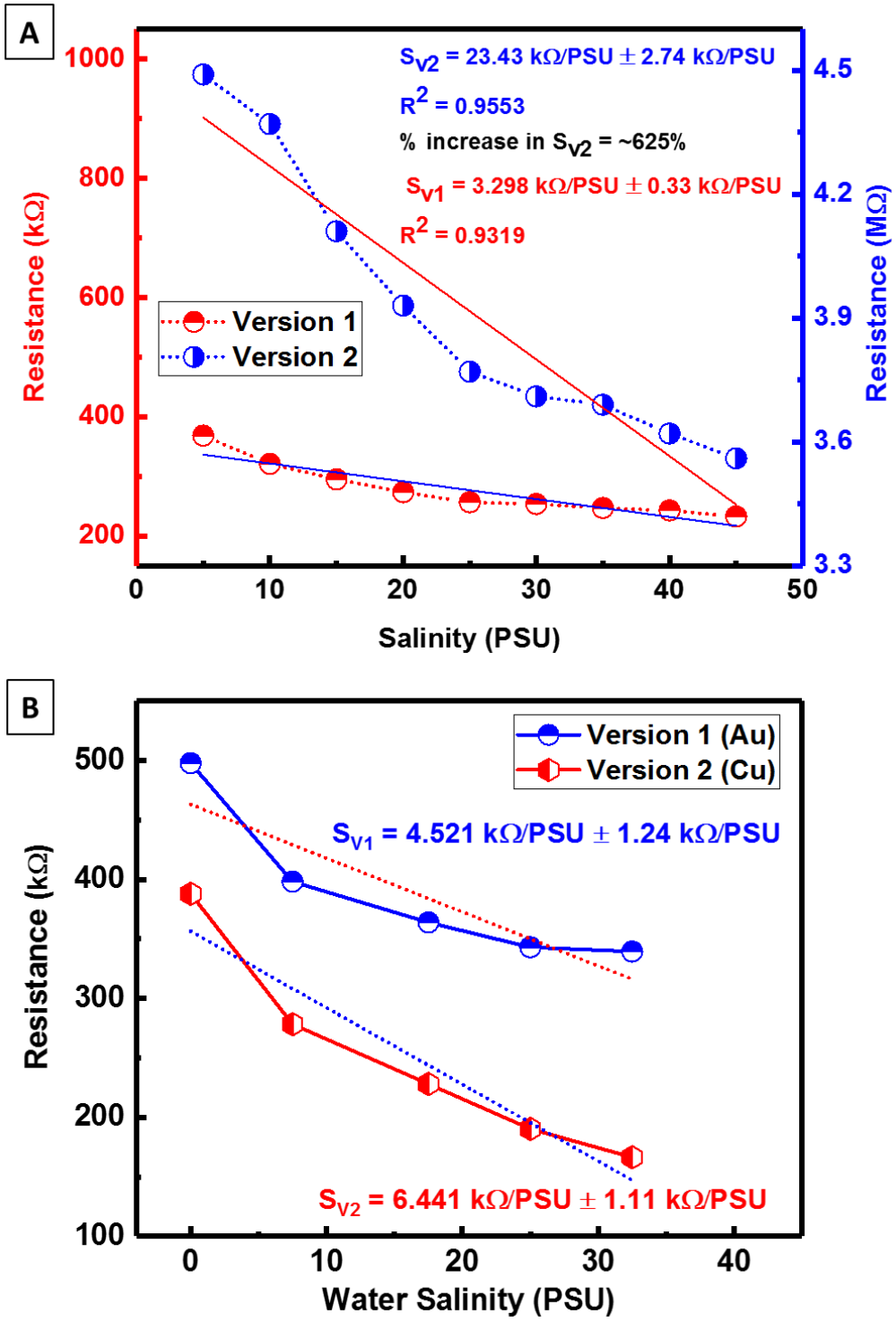

Figure S2: Comparison of the performance of (A) previous version and present version water salinity sensor for improved sensitivity by modified design, and (B) Present version comparison

for two different material choices of Au and Cu. An increase of ~625% sensitivity is observed due to design modification, while increase in sensitivity has been neglected.

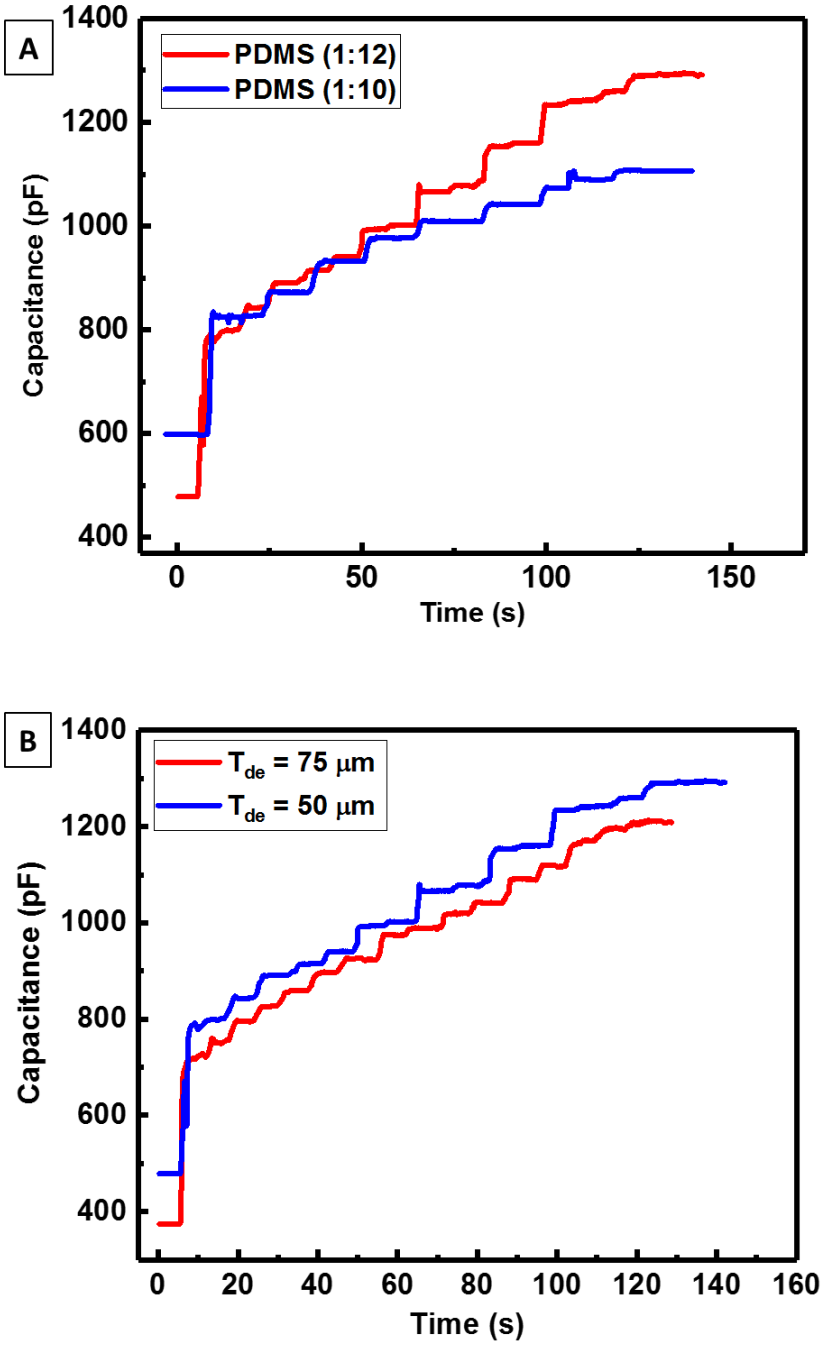

Figure S3: Dielectric material optimisation for pressure increasing the pressure sensitivity and the range of depths that can be measured. (A) Effect of the variation in the mixing ratio of PDMS elastomer to curing agent, with (12:1) ratio showing higher sensitivity due to increased

compressibility. (B) Effect of dielectric thickness variation on sensitivity and absolute values, optimum thickness is 50 µm.

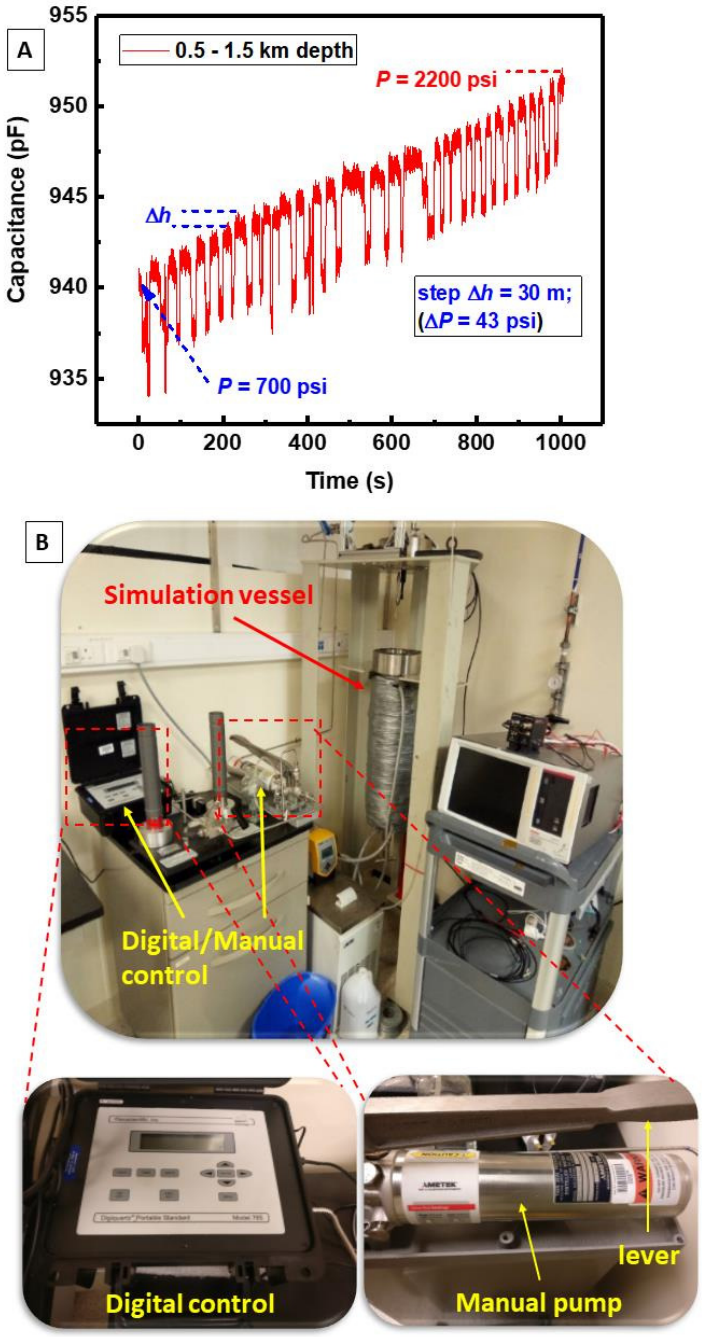

Figure S4: Harsh marine environment real-time pressure recording using version 2 Marine Skin platform, (A) demonstrating linear increment with the increased pressure, high sensitivity, resolution and fast response time by observed oscillations due to manual handling. (B)

Experimental setup for the high-pressure simulation and testing in the central labs (inset shows magnified images of digital control for temperature and pressure (left black box) and manual control unit for pressure using a hydraulic pump pumped using a manual handheld lever. A dead weight analog reading is also visible that looks like poles in B.

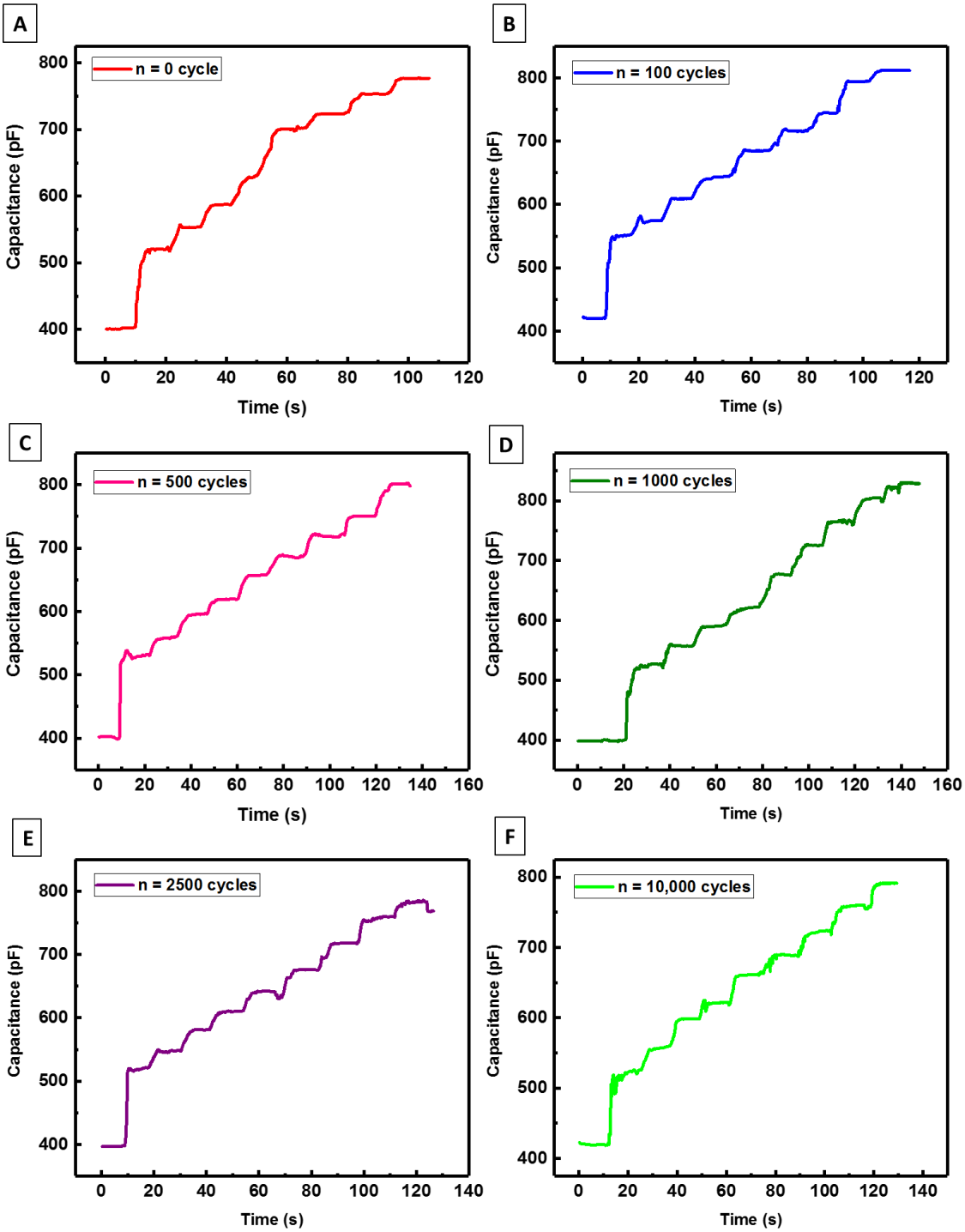

Figure S5: Real-time depth measurements over multiple bending cycles. Measurements are recorded after subjecting sensor to the multiple bending cycles (A)-(F) from 0 to 10,000 cycles. Real-time measurements of change in capacitance with increasing pressure (due to incremental depth) are observed with similar sensitivities.

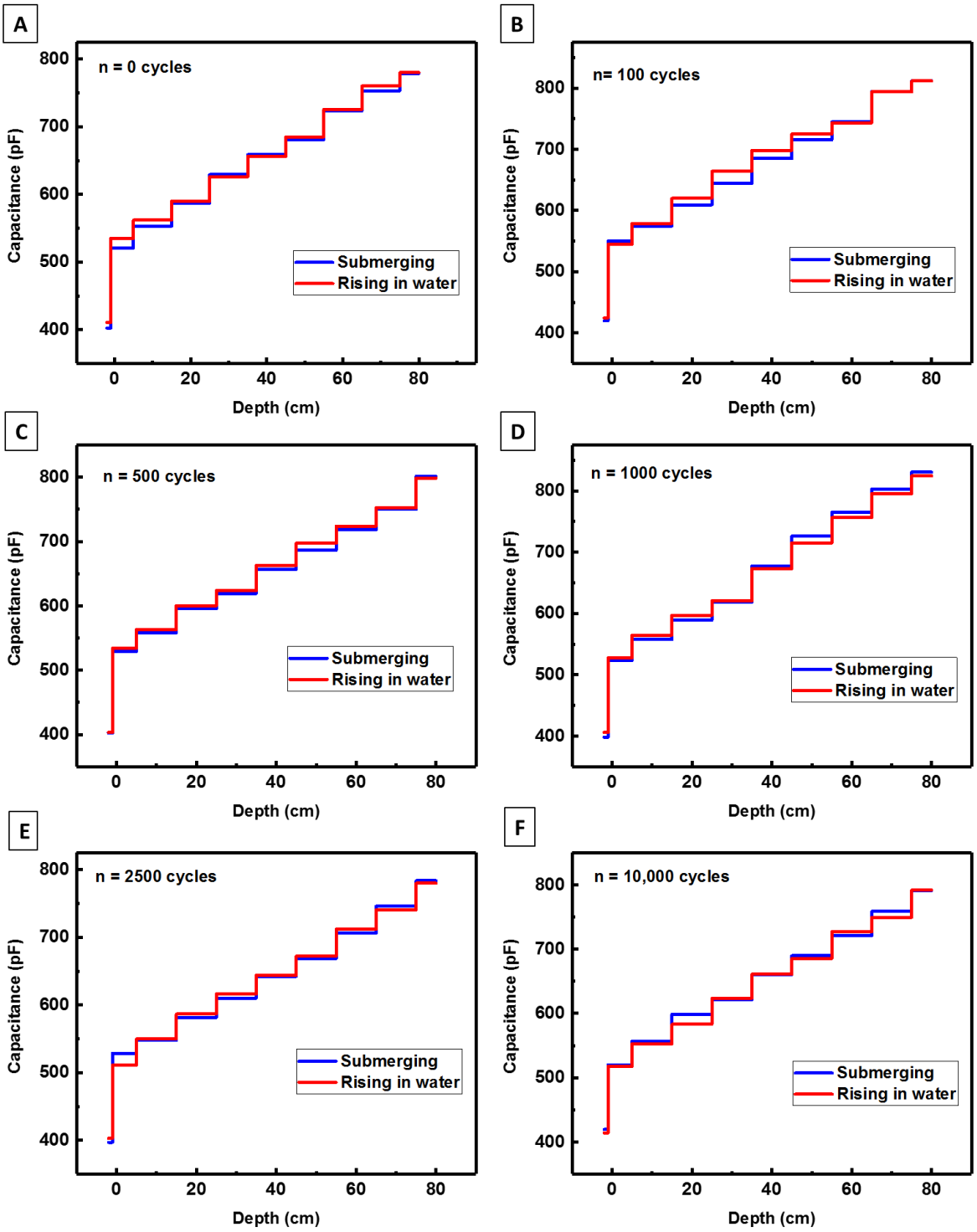

Figure S6: Robustness of the pressure sensor characterized for the pressure sensor when subjected to extreme bending cycle test of (1 mm bending radii) (A) - (F) with 0, 100, 500, 1000, 2500, and 10 thousand cycles respectively. Discrete measurements are plotted at step heights of ~10 cm for observing the hysteresis during submerging and rising from the water in the acrylic tank.

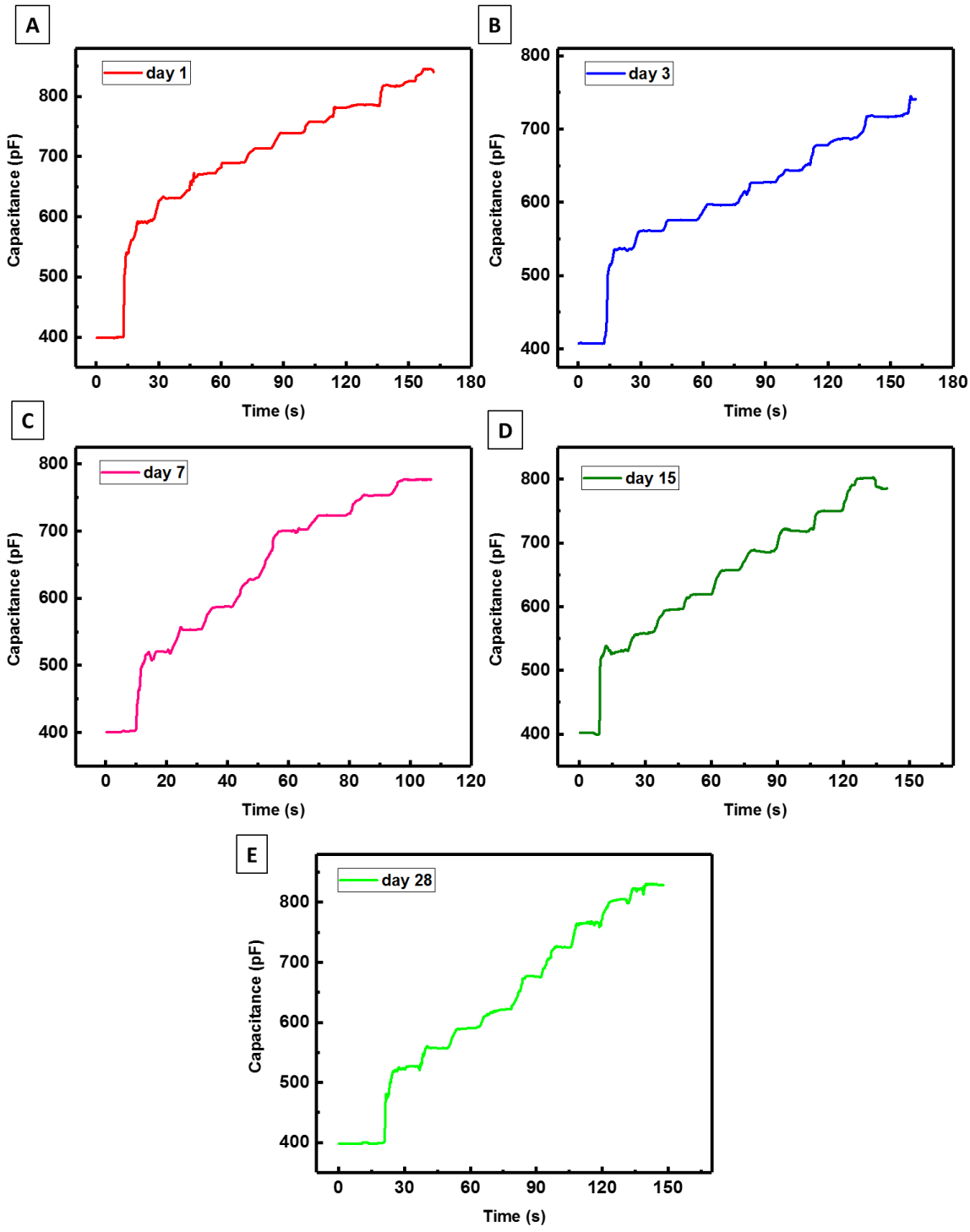

Figure S7: Real-time depth measurements against the time while submerging the sensors in the seawater in steps of 10 cm to observe the effect of prolonged exposure to saline water. (A) – (E) Devices were characterized after 1 day, 3 day, 7, 15, and 28 days of immersion in the Red sea water (41 PSU) and has observed no significant change in performance.

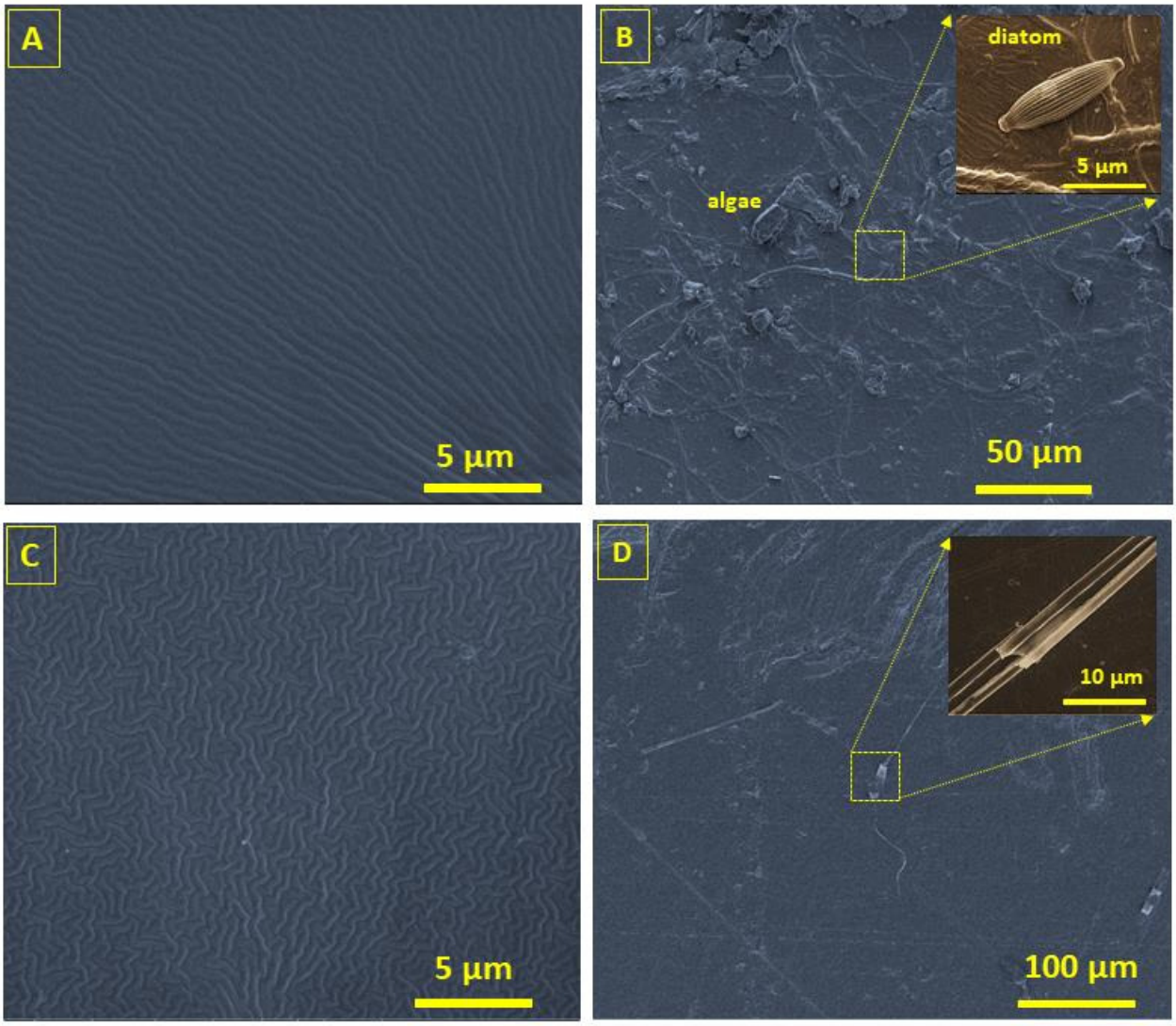

Figure S8: Scanning electron microscopic (SEM) images of the soft-polymeric encapsualted packaging for studying the biofouling effect. Samples has been submerged in the Red sea water for 6 weeks and then a standrad process was followed to fix any kind of biological traces on the sample followed by acquiring the SEM images. SEM of blanket PDMS showing different textures (A) before and (C) after O_2 plasma treatment for samples to be immersed in water. (B) sample 1 showing development of algea and salt accumulation with a few traces of diatoms (inset) after 6 weeks of constant sumbersion in the Red seawater. And (D) the significant reduction in the biofouling development due to treatment and weak adhesion forces of the biofouling organisms that are self-released by drag forces within the water stream.

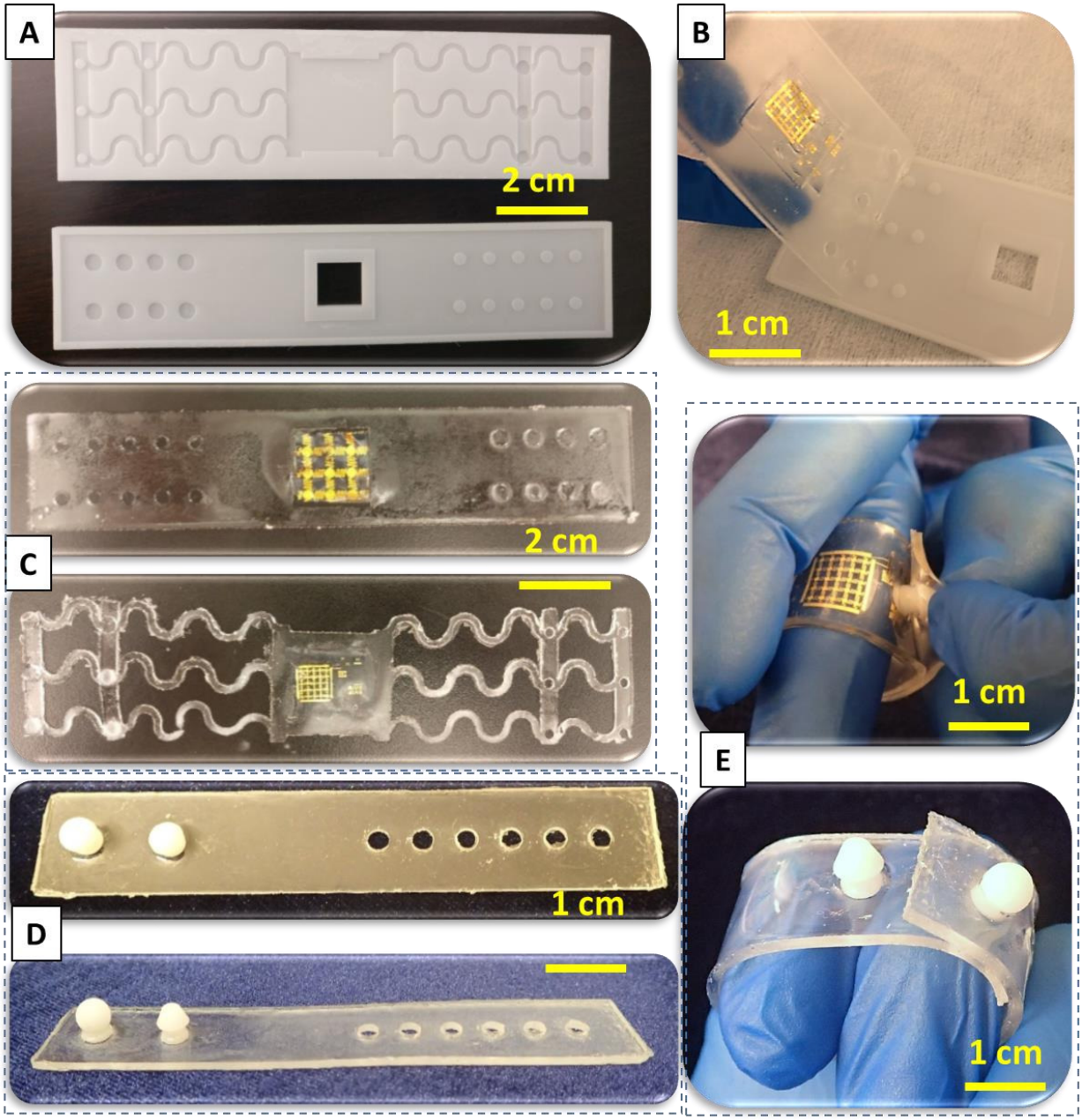

Figure S9: (A) 3D printed mold designs for multiple wearable bracelet. (B) Easy peeling-off of the flexible and stretchable bracelet from the 3D mold, (C) two designs having Marine Skin embedded within the bracelet with soft-mushroom pins to hold. Serpentine structures (bottom) can provide more breathability for animal and stretchability to the bracelet. (D) Modified bracelet design with 3D printed mushroom pins (spherical and trapezoidal shape) to improve inter-locking mechanism. (E) Increased inter-locking strength due to the incorporation of 3D printed mushroom pins has little effect on the flexibility.